ORNL/TM-10047

ornl

OAK RIDGE NATIONAL LABORATORY

MARTIN MARIETTA

Scintillation Light Transport and Detection

T. A. Gabriel
R. A. Lillie

OPERATED BY
MARTIN MARIETTA ENERGY SYSTEMS, INC.
FOR THE UNITED STATES
DEPARTMENT OF ENERGY

Printed in the United States of America. Available from
National Technical Information Service
U.S. Department of Commerce
5285 Port Royal Road, Springfield, Virginia 22161
NTIS price codes—Printed Copy A02 Microfiche A01

ORNL/TM-10047

Engineering Physics and Mathematics Division

Scintillation Light Transport and Detection*

T. A. Gabriel and R. A. Lillie

*Submitted for Journal publication

Date Issued: August 1986

Research sponsored by
Office of High Energy and Nuclear Physics
U.S. Department of Energy

Prepared by the
Oak Ridge National Laboratory
Oak Ridge, Tennessee 37831
operated by
Martin Marietta Energy Systems, Inc.
for the
U.S. DEPARTMENT OF ENERGY
under Contract No. DE-AC05-840R21400

Abstract

The MORSE neutron gamma-ray transport code has been modified to allow for the transport of scintillation light. This modified code is used to analyze the light collection characteristics of a large liquid scintillator module ($18 \times 18 \times 350$ cm^3).

I. Introduction and Method of Calculation

Efficient collection of scintillation light produced by the energy deposition of a charged particle is important in the overall performance of a scintillator detector system. The detection efficiency is determined by many factors including the geometry of the modular section, the index of refraction of the scintillator material and external material (usually air)* which determines the internal reflection characteristics, the absorption length of scintillation light, the photoelectron conversion efficiency of the phototubes, and the size of the phototubes. The MORSE[1] Monte Carlo code was modified to include all of the above factors so that accurate scintillation light transport could be carried out.

The wavelength distribution of the isotropically distributed scintillation light is shown in the upper graph of Fig. 1. The wavelength distribution was used by employing standard sampling techniques to define the source wavelength for the transport calculation. As implied by the histogram in Fig. 1, the calculation was carried out using 15 scintillation light wavelength groups, each group being 10 nm wide.

The absorption length for all wavelengths of light considered was assumed to be 75, 150, or 225 cm. Three sets of 15-group cross sections (reflecting the above absorption lengths) with no downscatter were generated. During the transport, scintillation light which traveled the sampled flight path before reaching the phototube was assumed to be absorbed and therefore would not contribute to the detector response.

Scintillation photons which reached the sides of the modules were allowed to either escape or undergo specular reflection. Any photon whose angle of incidence was greater than the critical angle was internally reflected. Any photon whose angle of incidence was less than the critical angle was allowed to escape from the system and therefore would not contribute to the detector response.† The critical angle is defined from the following expression: $\sin\theta = 1/n$, where θ = angle of photon relative to the normal at the surface and n = the index of refraction of the scintillator material which for these calculations has been taken to be 1.5.

Scintillation photons which are not absorbed or do not leak from the system reach the phototubes (represented by the 2 cylindrical holes in the geometry) and can produce a detectable photoelectron. The probability of this occuring is given by the bottom graph in Fig. 1. Analytically, these data can be represented by the following expression: $\epsilon = 0.26\, e^{-5.2\mathrm{x}10^{-5}(\lambda - 400.)^2}$. Generally speaking, most phototubes are approximately 20-25% efficient, requiring 4 to 5 scintillation gamma rays to produce one photoelectron.

---

*Generally for liquid scintillator systems, the box, usually lucite, containing the liquid has an index of refraction very similar to that of the scintillator. Internal reflection will then occur at the box/air interface and not at the scintillator/box interface.

†Some reflection is possible due to surface irregularity contamination for angles less than the critical angle. However, this effect is neglected in these calculations.

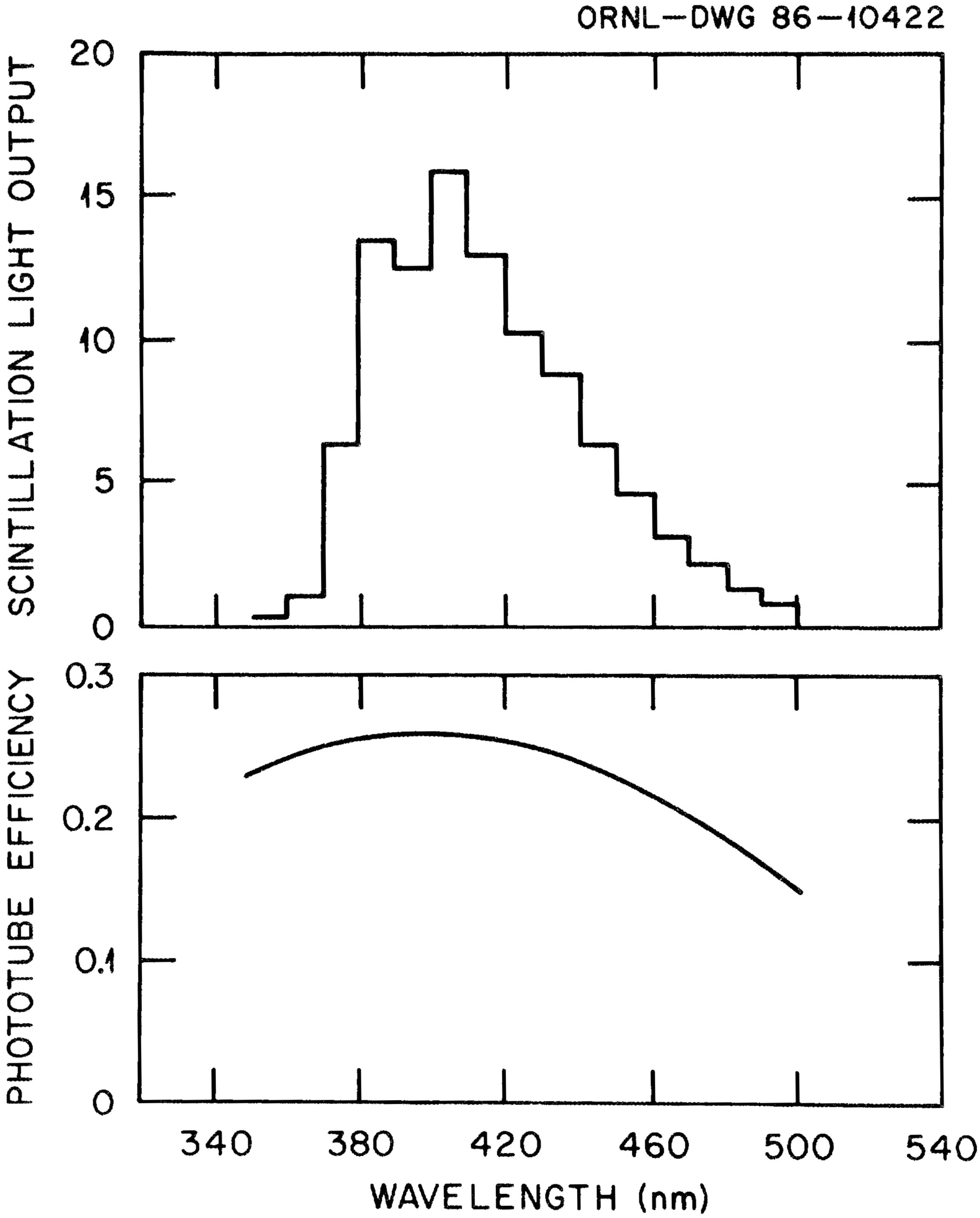

Fig. 1. Scintillation light output and phototube efficiency versus wave length.

No statistical weighting was used in any of these calculations. A source particle which started with a weight of one had a statistical weight of one when or if it finally produced a photoelectron at the phototube. Statistical weighting would have yielded the same average results, but with these calculations analog fluctuations are also necessary if the detector efficiency with respect to light collection is to be properly determined.

The detector module size considered for these calculations is 18.3x18.3x300.3 cm^3 (x, y, z coordinates were chosen such that 0, 0, 0 represented the center of the module).* The wall thickness of the container is 0.15 cm which yields an active scintillator volume of 18.x18.x300. cm^3. Attached at each end of the detector is a 7.62 cm diameter phototube. The geometry of the detector module was set up using the combinatorial geometry package in MORSE. The phototubes were represented by a cylindrical hole cut into each end (z = ±150.) of the module.

II. Results

The number of photoelectrons produced in both phototubes as a function of the number of source scintillation photons and as a function of scintillation photo absorption length is given in Fig. 2. These results are for a source of photons located in the center of the detector module. As can be seen, only a small number of photoelectrons are produced relative to the number of initial scintillation photons. A fit to these curves yields the following expressions:

$$PE = \begin{cases} 1.125\text{x}10^{-3}\,S \text{ for } \lambda = 75 \text{ cm} \\ 4.113\text{x}10^{-3}\,S \text{ for } \lambda = 150 \text{ cm} \\ 6.688\text{x}10^{-3}\,S \text{ for } \lambda = 225 \text{ cm} \end{cases}$$

where S is the number of scintillation photons and PE is the number of produced photoelectrons.

For liquid or plastic scintillator approximately 100-125 eV of energy deposition is required to produce one scintillation photon. Therefore, 4000 photons correspond to 0.4-0.5 MeV in energy deposition. Figure 2 defines the energy normalization for the detector module. Over the range covered by these calculations, the response is very linear with respect to energy deposition.

The energy resolution of the detector module was determined not by the average number of photoelectrons produced, but by the fluctuations in the number produced. An example of these fluctuations is illustrated in Fig. 3 for 2000 source scintillation photons located in the center of the module. The solid curve was obtained directly from the calculated data and the dashed curve was obtained from a Gaussian ($\alpha e^{-(x-x_o)^2/2\sigma^2}$) fit to the data. The data are very well fitted by a Gaussian curve. The fluctuation as measured by the standard deviation σ as a function of scintillation gammas is given in Fig. 4. As

*This detector module is being constructed for use at the KfK/SNS neutrino experiment.

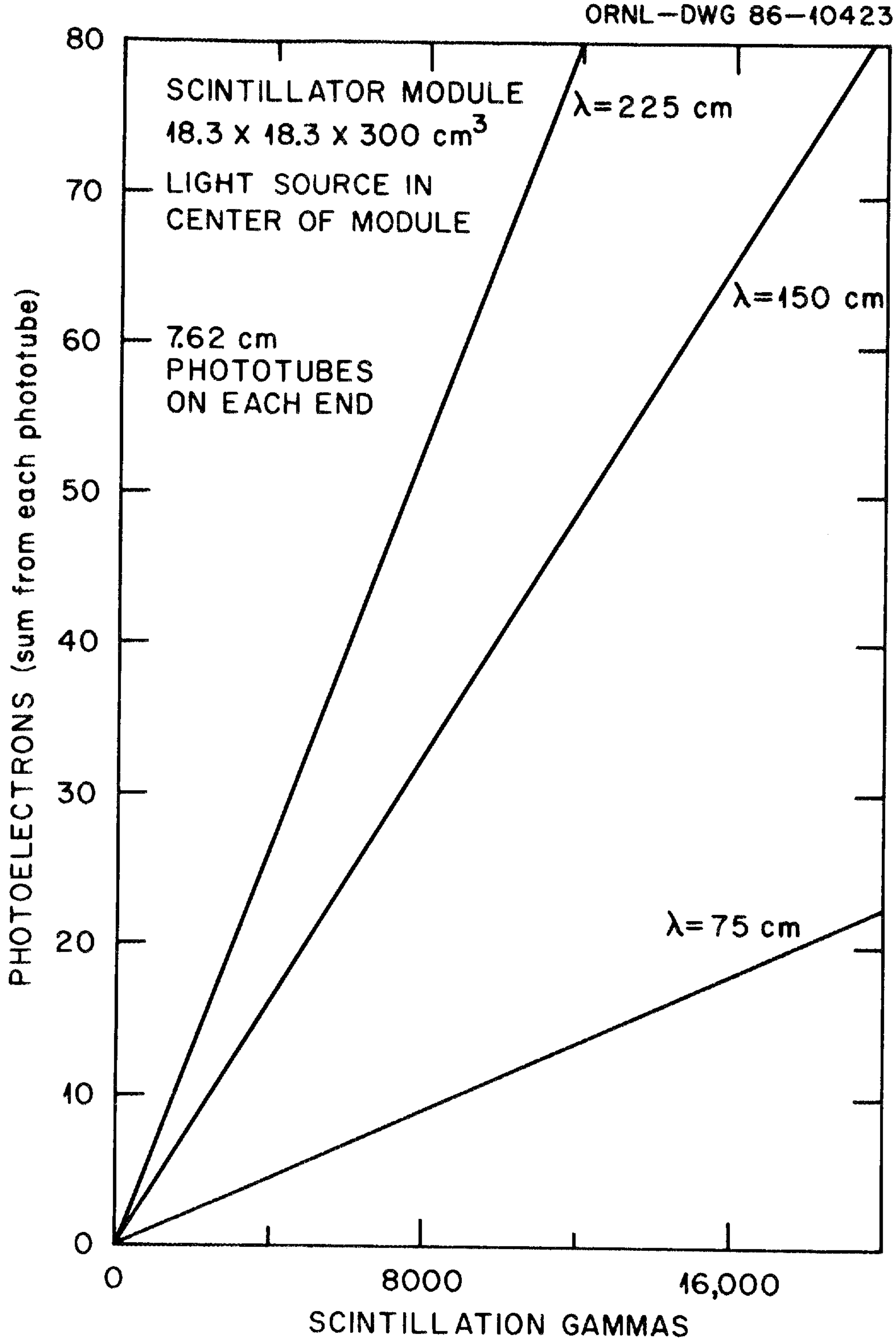

Fig. 2. **The number of photoelectrons produced versus the number of source scintillation photons.**

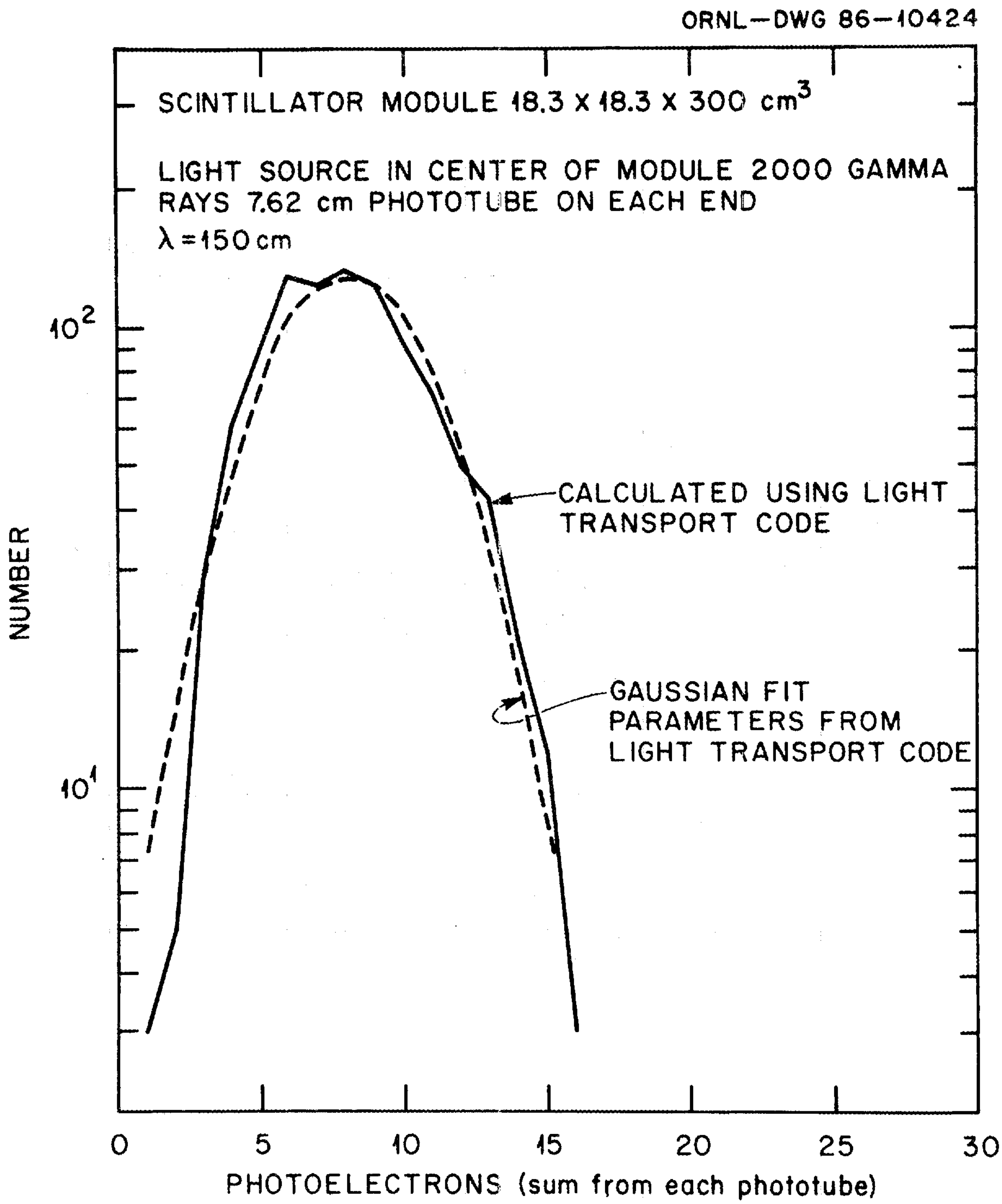

Fig. 3. Comparison between calculated fluctuation data and a Gaussian fit to these data.

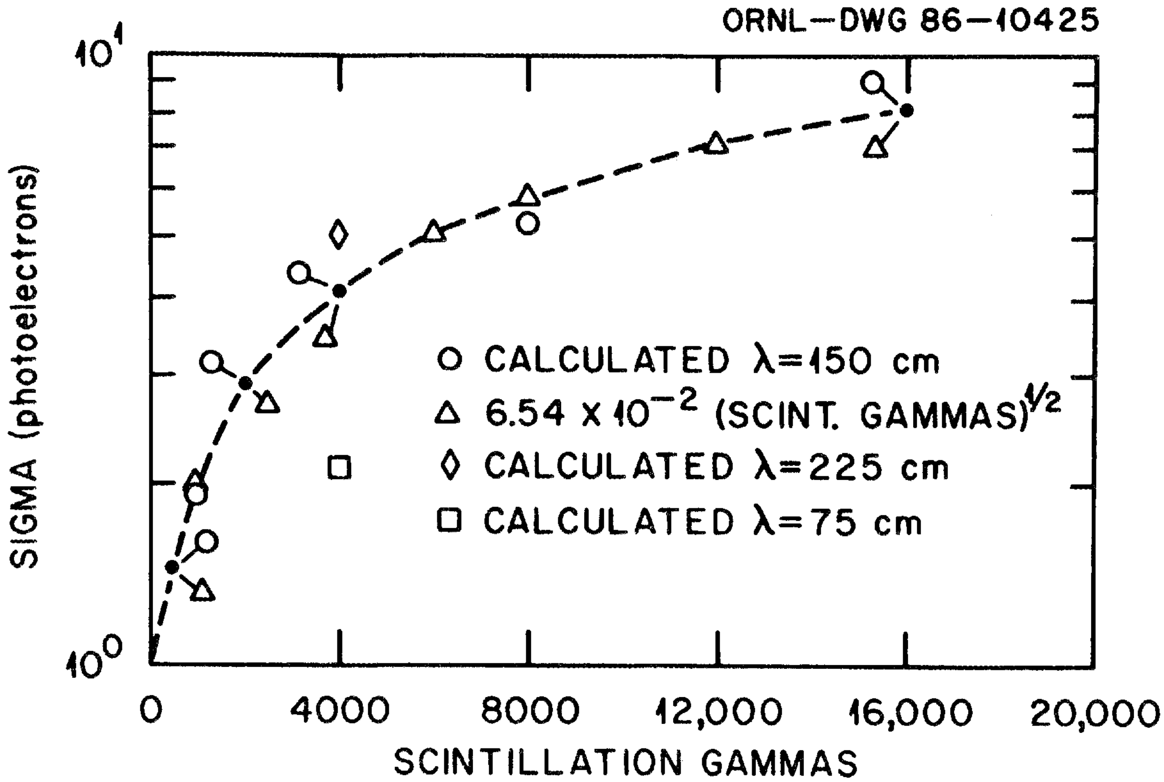

Fig. 4. Standard deviation in the number of photoelectrons produced versus the number of scintillation photons.

one would expect from statistical theory, the curve in Fig. 4 is proportional to the square root of the number of photons. A best fit to the data yields the following expression: $\sigma = 6.54\text{x}10^{-2}\ S^{1/2}$ for $\lambda = 150$ cm and S is the number of scintillation photons. Data points for $\lambda = 75$ and 225 cm are also given. However, by using the data in Fig. 2, the data for $\lambda = 150$ cm can be used to obtain σ's for $\lambda = 75$ and 225 cm. For example, 4000 photons for $\lambda = 75$ cm correspond to approximately 1200 photons for the $\lambda = 150$-cm case relative to the number of photoelectrons produced. Comparing these values in Fig. 4 yields the same σ.

The data presented so far have been for an isotopic source located in the center of the module. The spatial variation of the average number of photoelectrons detected as a function of distance from the center of the detector module toward one of the phototubes is given in Fig. 5. The coordinates (x,y) remain on axis. A strong variation in the average number is evident for all absorption lengths especially as the edge of the module is approached. Ideally, these curves should be as flat as possible. By using timing differences between the two phototubes to locate the energy deposition site and the above curves, the spatial variation of light collection as it influences energy resolution can be partially minimized.

Calculations have also been carried out to determine the variation in signal when the source is moved along the x-axis and the y and z coordinates are fixed. This variation in source location leads to very small changes, except at the very edge of the active scintillator region and should not lead to any serious resolution degradation. Fluctuations in the data presented in Fig. 5 can be obtained from the the data given in Figs. 2 and 4. Similar data are presented in Fig. 6 as were given in Fig. 5 except that only one phototube has been considered.

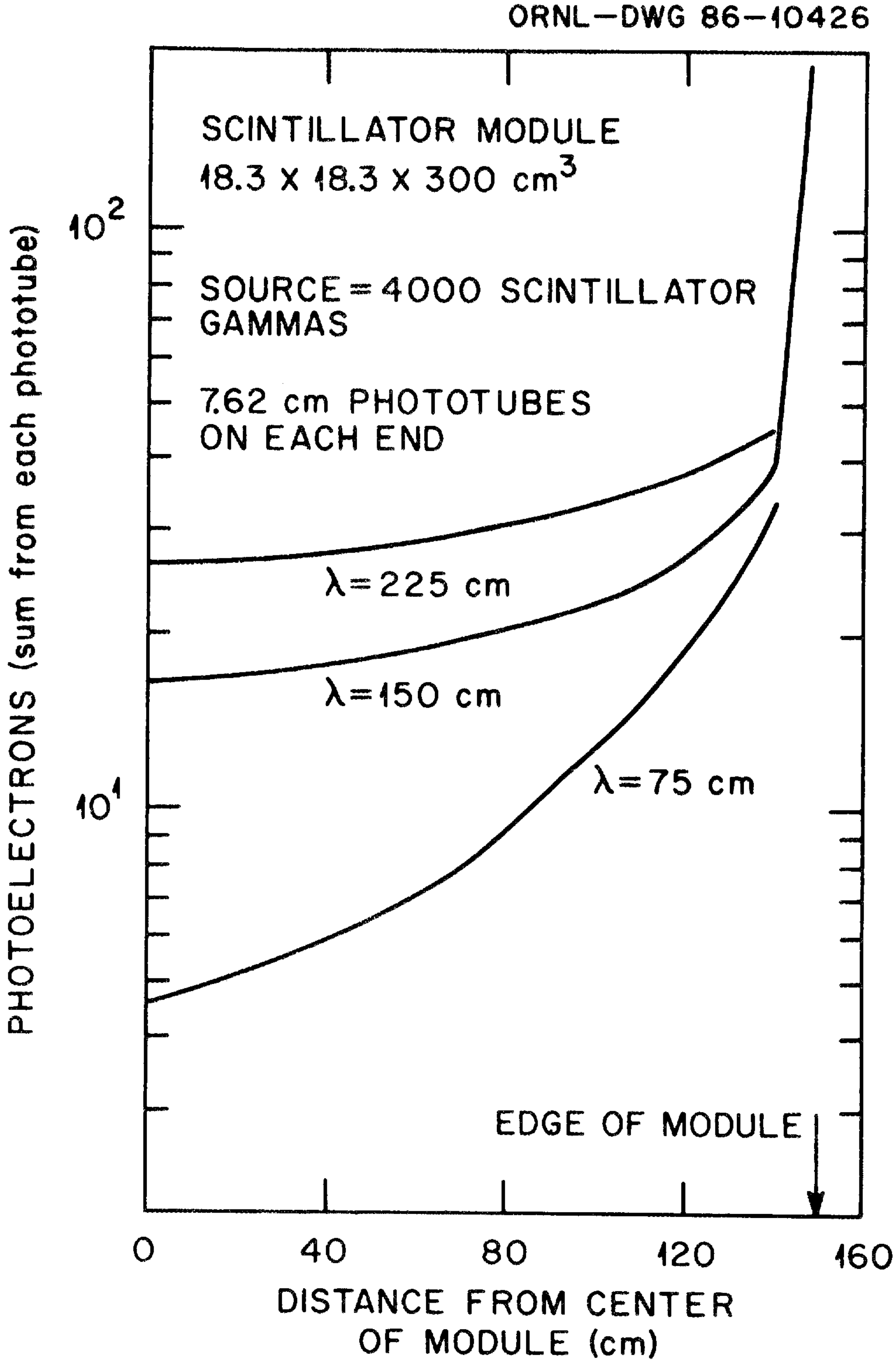

Fig. 5. Spatial variation in the number of photoelectrons produced as a function of distance from the center of the module.

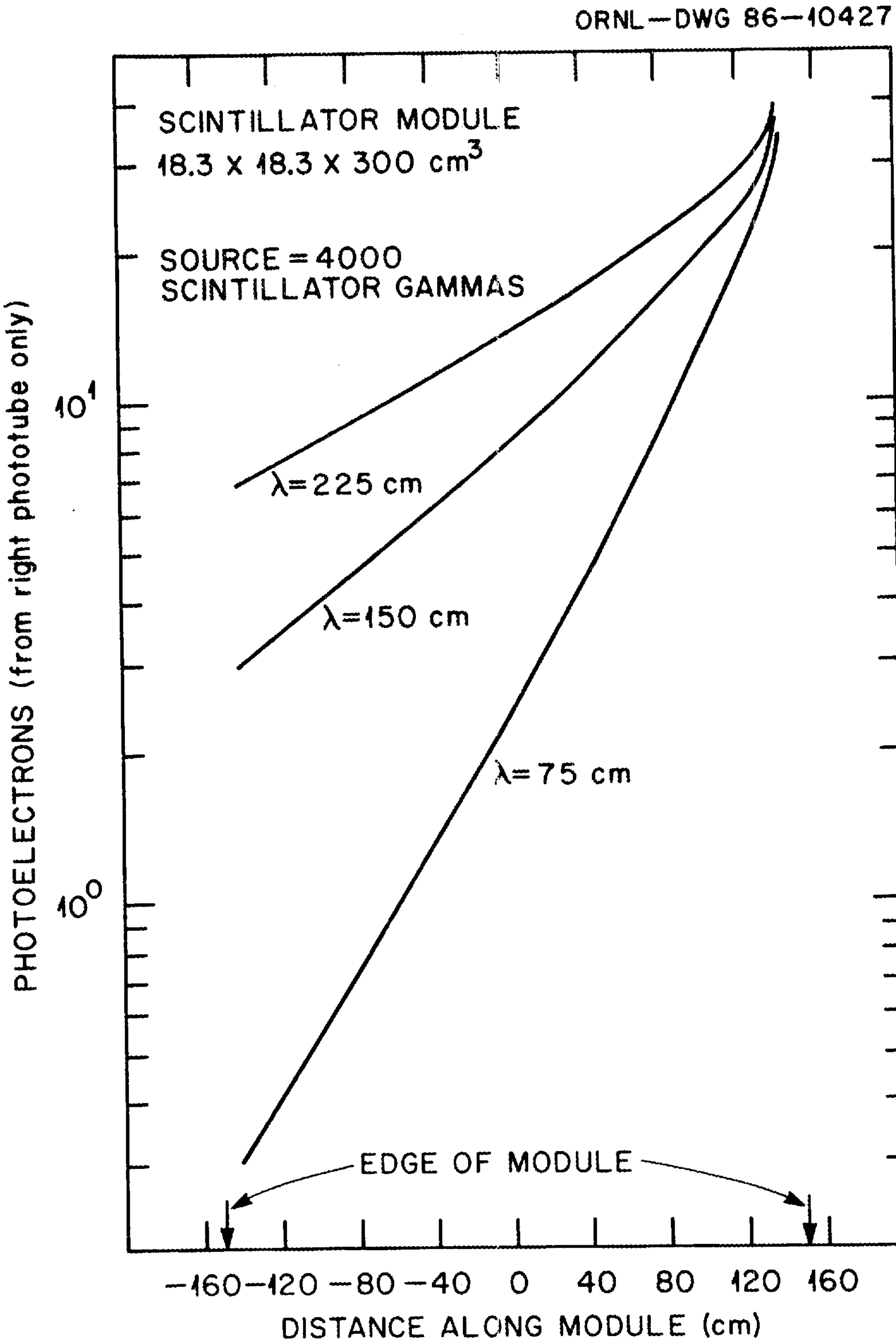

Fig. 6. Spatial variation in the number of photoelectrons produced in one phototube only as a function of distance from the center of the module.

REFERENCES

1. M. B. Emmett, "The MORSE Monte Carlo Radiation Transport Code System," ORNL/TM-4972 (February 1975).

INTERNAL DISTRIBUTION

1. L. S. Abbott
2. F. S. Alsmiller
3. R. G. Alsmiller, Jr.
4–8. B. L. Bishop
9–12. T. A. Gabriel
13–14. R. A. Lillie
15. F. C. Maienschein
16. R. W. Peelle
17. RSIC
18. R. T. Santoro
19. A. Zucker
20. P. W. Dickson, Jr. (Consultant)
21. G. H. Golub (Consultant)
22. R. Haralick (Consultant)
23. D. Steiner (Consultant)
24–25. Central Research Library
26. ORNL Y-12 Technical Library
Document Reference Section
27–28. Laboratory Records
29. ORNL Patent Office
30. Laboratory Records - RC

EXTERNAL DISTRIBUTION

31. Office of Assistant Manager for Energy Research & Development, DOE-ORO, Oak Ridge, TN 37830

32. Argonne National Laboratory, Library Services Department, 302-CE125, 9700 S. Cass Avenue, Argonne, IL 60439

33. T. W. Armstrong, Science Applications, Inc., PO Box 2807, La Jolla, CA 92038

34. Miguel Awschalom, National Accelerator Laboratory, PO Box 500, Batavia, IL 60510

35. V. S. Barashenkov, Laboratory of Theoretical Physics, Joint Institute for Nuclear Research, Head Post Office, PO Box 79, Moscow, USSR

36. Dr. Gerald W. Bennett, Brookhaven National Laboratory, Upton, NY 11973

37. D. Berley, National Science Foundation, Washington, DC 20550

38. Dr. Elliott Bloom, Stanford Linear Accelerator Center, PO Box 4349, Stanford, CA 94305

39. Brookhaven National Laboratory, Attention: Research Library, Upton, NY 11973

40. Dr. Bruce Brown, Fermi National Accelerator Laboratory, PO Box 500, Batavia, IL 60510

41. Dr. David O. Caldwell, Department of Physics, University of California at Santa Barbara, Santa Barbara, CA 93106

42. Stanley B. Curtis, Lawrence Radiation Laboratory, Bldg. 29, Room 213, Berkeley, CA 94720

43. Anna Di Cicacco, Exp. VA1, CERN, CH1211, Geneva, Switzerland.

44. Herbert Destaebler, Stanford Linear Accelerator Center, Stanford University, Stanford, CA 94305

45. R. D. Edge, Physics Department, University of South Carolina, Columbia, SC 29208

46. Dr. R. Eisenstein, Department of Physics, University of Illinois, Urbana, IL 61801

47. R. W. Ellsworth, George Mason University, Fairfax, VA 22030

48. Dr. Chris Fabjan, CERN, Geneva 23, Switzerland

49. Dr. G. Feldman, Stanford Linear Accelerator Center, Stanford University, Stanford, CA 94305

50. Dr. W. T. Ford, Experiment 1A-Lab C, Fermi National Accelerator Laboratory, PO Box 500, Batavia, IL 60510

51. Dr. E. Fowler, Department of Physics, Purdue University, West Lafayette, IN 47907

52. H. T. Freudenreich, University of Maryland, College Park, MD 20742

53. E. Freytag, Deutsches Elektronen-Synchrotron, DESY, 2 Hamburg Dr., Flottbek, Notkesteig 1, W. Germany

54. Dr. G. T. Gillies, Department of Physics, University of Virginia, Charlottesville, VA 22901

55. Dr. Gary E. Gladding, University of Illinois, Department of Physics, Urbana, IL 61801

56. K. Goebel, Health Physics Group, CERN, 1211 Geneva 23, Switzerland

57. J. A. Goodman, University of Maryland, College Park, MD 20742

58. Dr. M. Goodman, Department of Physics, Harvard University, Cambridge, MA 02138

59. Dr. Herman Grunder, Deputy Director, General Sciences, Lawrence Berkeley Laboratory, Bldg. 50A, Room 4119, 1 Cyclotron Rd., Berkeley, CA 94720

60. Frenc Hajnal, Health and Safety Laboratory, U.S. Department of Energy, 376 Hudston St., NY, NY 10014

61. Dr. D. Hitlin, Stanford Linear Accelerator Center, Stanford University, Stanford, CA 94305

62. M. Hofert, CERN, 1211 Geneva 23, Switzerland

63. Mr. Terrence Jensen, Dept. of Physics and Astronomy, The University of Rochester, Rochester, NY 14627

64. Dr. Inga Karliner, Physics Dept., University of Illinois, Urbana, IL 61801

65. Prof. D. Lal, Tata Institute of Fundamental Research, National Centre of the Government of India for Nuclear Science & Mathematics, Homi Bhabha Rd., Bombay 5, India

66. Lawrence Livermore Laboratory, Technical Information Department, PO box 808, Livermore, CA 94550

67. V. Lebedev, Institute of High Energy Physics, Serpukhov, Moscow Region, USSR

68. Library for Nuclear Science, Massachusetts Institute of Technology at Middleton, Middleton, MA 01949

69. Dr. J. LoSecco, Department of Physics, California Institute of Technology, Pasadena, CA 91125

70. Dr. J. Marks, Accelerator Fusion Research Division, Lawrence Berkeley Laboratory, Bldg. 50, Room 149, 1 Cyclotron Rd., Berkeley, CA 94720

71. A. I. Mincer, University of Maryland, College Park, MD 20742

72. Dr. V. S. Narasimham, Tata Institute of Fundamental Research, Bombay 400 005, India

73. W. R. Nelson, Stanford Linear Accelerator Center, Stanford University, PO Box 4349, Stanford, CA 94305

74. Keran O'Brien, Health and Safety Laboratory, U.S. Department of Energy, 376 Hudson St., NY, NY 10014

75. Dr. T. R. Palfrey, Jr., Department of Physics, Purdue University, West Lafayette, IN 47907

76. Dr. Robert Palmer, Brookhaven National Laboratory, Upton, NY 11973

77. Dr. C. W. Peck, Department of Physics, California Institute of Technology, Pasadena, CA 91109

78. J. Ranft, Karl-Marx University, Physics Section, Linnestrasse 5, 701 Leipzig, W. Germany

79. Dr. Lincoln Reed, Division of High Energy and Nuclear Physics, Department of Energy, Washington, DC 20545

80. Dr. C. Rubbia, Lyman Laboratory, Harvard University, Cambridge, MA 02138

81. Dr. W. Schmidt, Institute of Experimental Nuclear Physics, University of Karlsruhe, 75 Karlsruhe, W. Germany

82. The Secretary, Radiation Group, Lab II, CERN, 1211 Geneva 23, Switzerland

83. Dr. Walter Selove, University of Pennsylvania, Department of Physics, Philadelphia, PA 19104

84. B. S. P. Shen, Department of Astronomy, University of Pennsylvania, Philadelphia, PA 19104

85. Dr. M. Shupe, Department of Physics, University of Minnesota, Minneapolis, MN 55455

86. Stanford Linear Accelerator Center, Attention: Library, PO Box 4349, Stanford, CA 94305

87. Dr. Alan Stevens, Accelerator Dept. Bldg. 911, Brookhaven National Laboratory, Upton, NY 11973

88. G. R. Stevenson, Radiation Protection Group, Lab II, CERN, 1211 Geneva 23, Switzerland

89. Dr. L. Sulak, Department of Physics, University of Michigan, Ann Arbor, MI 48109

90. R. F. Taschek, Los Alamos National Laboratory, P.O. Box 1663, Los Alamos, NM 87544

91. R. Tesch, DESY, Hamburg, Notkesteig 1, W. Germany

92. Ralph H. Thomas, University of California, Lawrence Radiation Laboratory, Health Physics Department, Bldg.72, Berkeley, CA 94720

93. V. D. Toneev, Laboratory of Theoretical Physics, Joint Institute for Nuclear Research, Head Post Office, PO Box 79, Moscow, USSR

94. S. C. Tonwar, University of Maryland, College Park, MD 20742

95. W. Turchinetz, Massachusetts Institute of Technology, R26-411, Cambridge, MA 02139

96. Dr. W. J. Willis, CERN, Geneva 23, Switzerland

97. Dr. D. Winn, Lyman Laboratory, Harvard University, Cambridge, MA 02138

98. Dr. J. Wilcznski, Nuclear Research Center, Karlsruhe, W. Germany

99. Dr. S. Yellin, Stanford University, Stanford Linear Accelerator Center, P.O. Box 4349, Stanford, CA 94305

100. G. B. Yodh, University of Maryland, College Park, MD 20742

101. Dr. B. Zeitnitz, Nuclear Research Center, Karlsruhe, W. Germany

102–128. Technical Information Center, PO Box 62, Oak Ridge,TN 37831